Distribution Agreement

In presenting this thesis or dissertation as a partial fulfillment of the requirements for an advanced degree from Emory University, I hereby grant to Emory University and its agents the non-exclusive license to archive, make accessible, and display my thesis or dissertation in whole or in part in all forms of media, now or hereafter known, including display on the world wide web. I understand that I may select some access restrictions as part of the online submission of this thesis or dissertation. I retain all ownership rights to the copyright of the thesis or dissertation. I also retain the right to use in future works (such as articles or books) all or part of this thesis or dissertation.

Signature:

_____ _____

Lei Chu Date

Synthesis and Reactivity of Transition Metal Complexes Supported by a Neutral Tetraamine Ligand Containing *N,N'*-dimethylaniline Units

By

Lei Chu
Master of Science

Chemistry

Cora E. MacBeth, Ph.D.
Advisor

Craig L. Hill, Ph.D.
Committee Member

Simon B. Blakey, Ph.D.
Committee Member

Accepted:

Lisa A. Tedesco, Ph.D.
Dean of the James T. Laney School of Graduate Studies

Date

Synthesis and Reactivity of Transition Metal Complexes Supported by a Neutral Tetraamine Ligand Containing *N,N'*-dimethylaniline Units

By

Lei Chu
B.S. University of Science and Technology of China, 2006

Advisor: Cora E. MacBeth, Ph.D.

An abstract of
A thesis submitted to the Faculty of the
James T. Laney School of Graduate Studies of Emory University
in partial fulfillment of the requirements for the degree of
Master of Science
in Chemistry
2010

Abstract

Synthesis and Reactivity of Transition Metal Complexes Supported by a Neutral Tetraamine Ligand Containing *N,N'*-dimethylaniline Units

By Lei Chu

A novel ligand tris(2-dimethylaminoaryl)amine, L^{Me}, has been shown to coordinate with some first row transition metals to produce firve-coordinate complexes with distorted trigonal bipyramidal coordination geometry. For $[Co(L^{Me})Br]BPh_4$, $[Ni(L^{Me})Cl]BPh_4$, $[Fe(L^{Me})Cl]BPh_4$ and $[Cu(L^{Me})Cl]BF_4$, comparisons have been made to structures of related neutral ligand tris(2-dimethylaminoethyl)amine, Me_6tren. The results suggest that the more distorted geometries of $[M(L^{Me})X]^+$ complexes are due to the small chelate bite angle imposed by the rigid *o*-phenylenediamine ligand backbone. Spectroscopic and magnetic studies of these complexes are also described. The Cu(I)-carbonyl complexes $[Cu(L^{Me})(CO)]PF_6$ and $[Cu(Me_6tren)(CO)]PF_6$ have been prepared. Infrared spectroscopy investigations of these carbonyl complexes not only confirm that L^{Me} is a less neucleophilic ligand but also exhibit different solution and solid-state topologies. Finally, the reactivity of the $[Cu^I(L^{Me})]^+$ with dioxygen and the resulting species reactivity with C-H is bonds is described.

Synthesis and Reactivity of Transition Metal Complexes Supported by a Neutral Tetraamine Ligand Containing *N,N'*-dimethylaniline Units

By

Lei Chu
B.S. University of Science and Technology, 2006

Advisor: Cora E. MacBeth, Ph.D.

A thesis submitted to the Faculty of the
James T. Laney School of Graduate Studies of Emory University
in partial fulfillment of the requirements for the degree of
Master of Science
in Chemistry
2010

Table of Contents

List of Figures, Tables, Schemes, and Charts

Schemes **Page**

Charts **Page**

List of Abbreviations

ATRP: Atom transfer radical polymerization

Tren: tris(2-aminoethyl)amine

Me_6tren: tris(N,N'-dimethylaminoethyl)amine

TMPA: tris(2-pyridylmethyl)amine

L^{Me}: N(*o*-$PhNMe_2)_3$, tris(2-dimethylaminophenyl)amine

TBP: trigonal bipyramidal

SP: square pyramidal

THF: tetrahydrofuran

Et_2O: diethyl either

PhCHO: benzylaldehyde

$PhCH_2OH$: benzylalcohol

Part I. Transition Metal Complexes Supported by a Neutral Tetraamine Ligand Containing *N,N'*-dimethylaniline Units

I. I Introduction

Tripodal tetraamine ligands have been widely studies for several decades[1] because ancillary ligands play important role in regulating metal ion reactivity by influencing the geometric, steric and electronic features of the coordinated metal ions.[1-3] They have been utilized extensively in biomimetic copper[4-15] and iron[16-23] chemistry and as supporting scaffolds for copper mediated atom transfer radical polymerization (ATRP).[24-26] Some of the most familiar ligands in this class include this(2-aminoethyl)amine (tren), tris(N,N-dimethylaminoethyl)amine (Me6tren), and tris(2-pyridylmethyl)amine (TMPA) (Chart 1). Recent research in the areas of dioxygen activation by Cu(I)[4-6, 8, 11, 13, 27-29] and hydrogen peroxide activation by Fe(II)[16,30-32] complexes has demonstrated that the electronic and steric requirements of the tetraamine ligands play a crucial role in regulating the reactivity of these complexes. For example, Karlin and co-workers synthesized a series of electronically varied ligands based upon the TMPA scaffold by introducing various R group into the 4-pyridyl position of the ligand, $TMPA^{R}$ (where R = 4-pyridyl substituent).[33] In weakly coordinating solvents they found that the ligands with the greatest neuclophility (i.e., $TMPA^{OMe}$ and $TMPA^{NMe2}$) increased the thermodynamic stability of the resulting $[(TMPA^{R})Cu^{II}(O_2^{\cdot-})]^{+}$ and $[\{(TMPA)Cu^{II}\}_2(\mu\text{-}1,2\text{-}O_2^{2-})]^{2+}$ complexes and decreased the

dissociation rates of these species. These results were expected because dioxygen binding to Cu(I) centers is a redox process is a redox scaffolds. In other work, Britovsek and co-workers investigated the reactivity of a series of Fe(II) bis(triflate) complexes supported by neutral, tetraamine tripodal ligands with hydrogen peroxide as alkane oxidation catalysts.[16,32] They found that the solution-state structures of the bis(triflate) complexes and the mechanism of alkane oxidation was very dependent on the supporting ligands, and stronger field ligands containing two or more pyridyl groups favored six-coordinated species and prevented Fenton-type reaction chemistry.[16] Subsequent studies by these researchers using magnetic and spectroscopic studies confirmed that ligand rigidity and therefore catalysts stability under oxidizing conditions is a key determinate in the overall catalytic acivity of these species.

Chart 1. Common tripodal tetradentate tetraamine ligands

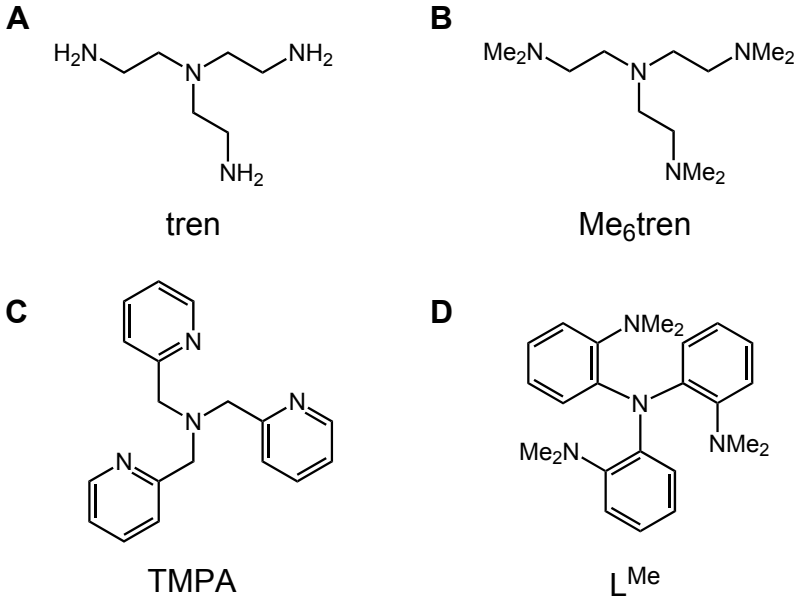

We recently reported the coordination chemistry of tris(2-dimethylaminophenyl)amine, N(*o*-$PhNH_2)_3$, a tripodal tetradentate ligand system that incorporates o-phenylenediamine donors into the ligand backbone, with Co(II).[34] We expected that incorporation of the o-phenylenediamine unit into a tripodal ligand would result in a more rigid tetraamine framework that could display non-innocent behavior.35 Further functionalization of tris(2-aminoaryl)amine to form trianionic tris(amidate)amine[34, 36-38] and tris(amido)amine ligands[38-41] has been described but neutral ligands based on the N(*o*-$PhNH_2)_3$ unit that lack reactive protons have remained unexplored. We synthesized N(*o*-$PhNMe_2)_3$, L^{Me} and explored the coordination chemistry of it. We described the synthesis, coordination chemistry and spectral properties of later, first-row transition metal ions supported by L^{Me}. The M^{II}-halide complexes, $[M^{II}(L^{Me})X]^+$, of this ligand have been compared to similar complexes supported by tris(2-dimethylaminoethyl)amine, Me_6tren. The spectroscopic and magnetic properties of the $[M^{II}(LMe)X]+$ series of complexes have been measured and used to provided information about the ligand field strength of LMe. Finally, the Cu(I) carbonyl complexes $[Cu(L^{Me})(CO)]+$ and $[Cu(Me_6tren)(CO)]+$ have been synthesized and characterized spectroscopically and used to probe the nucleophility of each ligand and to highlight differences in the coordination behaviors of these two ligands.

II. Results and Discussion

Synthesis

The neutral tetraamine ligand tris(2-dimethylaminoaryl)amine, N(*o*-PhNMe$_2$)$_3$ (L^{Me}), was synthesized in good yield by reductive methylation[42,43] of the primary amine precursor, N(*o*-PhNH$_2$)$_3$, (Scheme 1). The ligand can be recrystallized from hot methanol to yield analytically pure material. The L^{Me} scaffold was used to synthesize five, first-row transition metal complexes, including four cationic species with the general formula [M(L^{Me})X]$^+$ (where M=Fe^{II}, Co^{II}, Ni^{II} and Cu^{II} and X = Cl^- or Br^-). A general synthetic method for the Fe, Co, and Ni complexes is shown in Scheme 2.

In a standard metallation procedure, the ligand and anhydrous metal halide salt were stirred together in CH_2Cl_2. In situ, counter cation metathesis was then performed by treating the reaction mixture with one equivalent of $NaBPh_4$ as a methol solution. This procedure provides [Fe(L^{Me})Cl]BPh_4, [Co(L^{Me})Br]BPh_4, and [Ni(L^{Me})Cl]BPh_4 in good yields. The copper analogue, [Cu(L^{Me})Cl]BF_4, was synthesized in a similar manner except $AgBF_4$ was used in place of $NaBPh_4$. In addition to metallating the ligand with M^{II} ions, we were also interested in exploring coordination chemistry with Cu(I) due to the utility of neutral tetraamine ligands in Cu(I)-dioxygen chemistry. The Cu(I) complex, [Cu(L^{Me})]+, was synthesized by directly reacting [Cu(CH_3CN)$_4$]PF_6 with L^{Me} in anhydrous CH_3CN.

Scheme 1. Synthesis of the tris(2-dimethylaminoaryl)amine ligand (L^{Me})

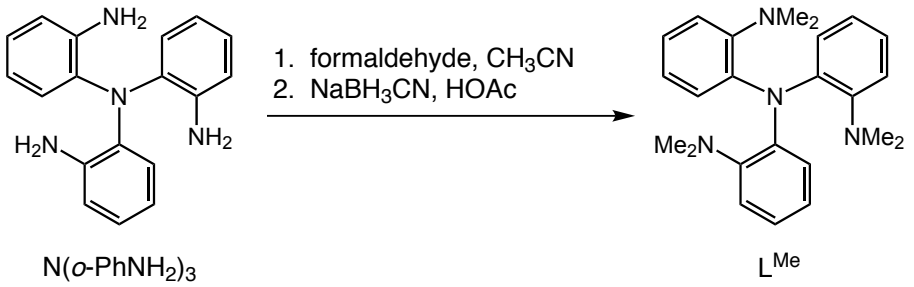

Scheme 2. Synthesis of $[M^{II}(L^{Me})X]BPh_4$ complexes

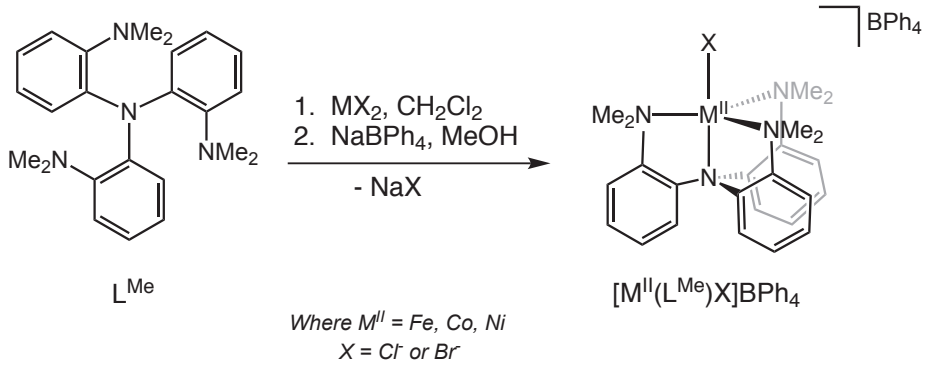

I.III X-ray Crystallographic Studies

X-ray quality crystals of L^{Me} could not be obtained, but the monoprotonated ligand salt, $[HL^{Me}]PF_6$, was readily recrystallized by diffusing diethyl ether into tetrahydrofuran solution. The molecular structure of the cation is shown in Figure 1. It shows the acidic proton (H1)

residing at one of the dimethylarylamine donors (N3). The acidic proton is also interacting with the other tertiary amine donors (N1 and N2) through hydrogen bonding interactions as evidenced by the close N3-N2 and N3-N1 through space distances of 2.932(3) and 2.797(3) Å, respectively. The pyramidalization of the apical N1 is approximately half-way between trigonal planar and tetrahedral as the sum of the C_{aryl}-N1-C_{aryl} bond angles is 346.3°. This type of pyramidalization is similar to what is observed in the solid-state structure of tris(2-hydroxyaryl)amine, N(*o*-$C_6H_4OH)_3$.[44]

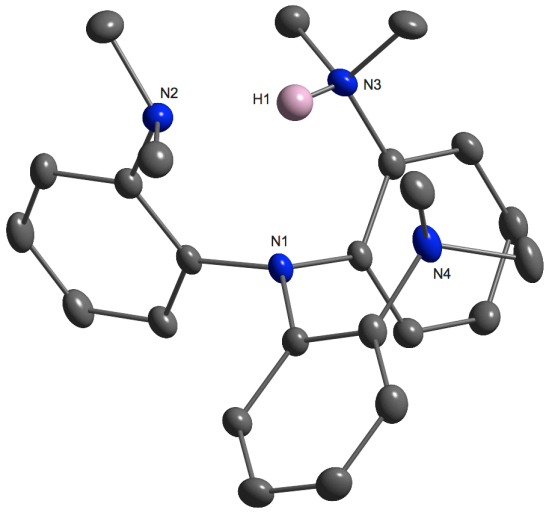

Figure 1. Thermal ellipsoid diagram of $[HL^{Me}]^+$. All of the hydrogen atoms except the acidic proton and the PF6- aion have been removed for clarity.

The Fe(II) complex, $[Fe(L^{Me})Cl]BPh_4$, was crystallized as pale yellow needles by diffusing diethyl ether into an CH_3CN solution of the complex. The molecular structure of $[Fe(L^{Me})Cl]^+$, as determined by X-ray diffraction, is shown in Figure 2A with selected bond lengths and angles listed in Table 1.The equatorial plane about the Fe is comprised of three dimethylarylamine ($PhNMe_2$) donor groups. The axial postions are occupied by Cl^- and the apical trisarylamine donor of the ligand backbone. The bond lengths and angles found in $[Fe(L^{Me})Cl]^+$ are similar to those observed in $[Fe(Me_6tren)Cl]^+$ (Figure 2B). For example, the average Fe-Neq bond lengths of 2.182(4) Å in [Fe(L^{Me})Cl]+ are slightly longer than 2.140(4) Å in [Fe(Me_6tren)Cl]+. The axial Fe-Cl bond length of 2.287(2) Å in $[Fe(LMe)Cl]^+$ is slightly shorter than 2.3149(16) Å in $[Fe(Me_6tren)Cl]^+$. The modest differences in axial bond lengths result in different degrees of distortions of Fe(II) ions from their respective equatorial planes. The Fe(II) center in [Fe(L^{Me})Cl]+ is positioned 0.45 Å above the equatorial plane while the Fe(II) center in [Fe(Me_6tren)Cl]+ is positioned 0.37 Å above the equatorial plane. The differences between the two structures can quantified by calculating the overall five-coordinate structural parameter (τ_5) displayed by the complexes (where τ_5 = 1.0 in an idealized trigonal bipyramidal environment (TBP) and τ_5 = 0 in an idealized square pyramidal geometry (SP)).[45] The Fe(II) center in [Fe(LMe)Cl]+ lies in a distorted TBP coordination geometry (τ_5 = 0.92), whereas the Fe(II) center in [Fe(Me_6tren)Cl]+ is held in a almost idealized TBP coordination gemotry (τ_5 = 1.0).

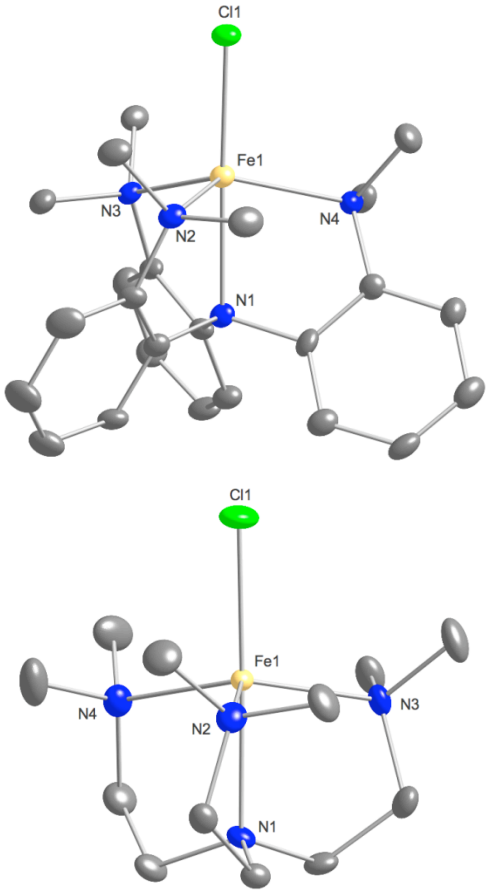

Figure 2. Molecular structures of $[Fe(L^{Me})Cl]^+$ and $[Fe(Me_6tren)Cl]^+$ (drawn at 30% probability). Aions and hydrogen atoms have removed for clarity.

Table 1. Selected bond lengths (Å) and angles (°) for $[Fe(L^{Me})Cl]BPh_4$ and $[Fe(Me_6tren)Cl]BPh_4$.

	$[Fe(L^{Me})Cl]^+$	$[Fe(Me_6tren)Cl]^+$
Fe1-Cl1	2.287(2)	2.3149(16)
Fe1-N1	2.241(4)	2.234(4)
Fe1-N2	2.179(4)	2.214(4)
Fe1-N3	2.177(4)	2.185(4)
Fe1-N4	2.190(4)	2.202(5)
N1-Fe-Cl1	177.15(11)	178.39(12)
N2-Fe-Cl1	99.76(12)	99.10(12)
N3-Fe-Cl1	104.43(10)	100.59(12)
N4-Fe-Cl1	101.76(13)	99.58(13)
N1-Fe-N2	78.60(15)	80.10(15)
N1- Fe-N3	78.37(13)	81.02(15)
N1- Fe-N4	77.31915)	79.65(16)
N2- Fe-N3	110.49(15)	116.58(16)
N3- Fe-N4	115.23(14)	116.33(16)
N2- Fe-N4	121.72(15)	118.67(16)

The structures of $[Co(L^{Me})Br]^+$, $[Ni(L^{Me})Cl]^+$, and $[Cu(L^{Me})Cl]^+$, were also determined by X-ray diffraction studies. The results of these studies are shown in Figure 3 and the metrical parameters for the three complexes are listed in Table 2. For $[Co(L^{Me})Br]BPh_4$, purple crystals were grown by slow diffusing diethyl ether into a concentrated CH_3CN solution. The Co^{2+} is positioned in an almost idealized trigonal TBP coordination environment (τ_5 = 1.0). The bond lengths of Co-N are very similar to those in structural similar $[Co(Me_6tren)Br]Br$ complex (τ_5 = 1.0).[25,26] For example, the Co-Br and average Co-N_{eq} bond lengths of 2.4167(4) Å and 2.1306(19) Å, respectively in $[Co(L^{Me})Br]^+$ are only slightly shorter than the corresponding bond lengths observed for $[Co(Me_6tren)Br]^+$ (Co-Br 2.4471(7) Å and Co-N_{eq} 2.137(2) Å). The Co-N_{ax} bond length (2.2280(18) Å) in $[Co(L^{Me})Br]^+$ is slightly elongated (~ 0.013 Å) compared to that in $[Co(Me_6tren)Br]^+$. The Co center in $[Co(L^{Me})Br]^+$ is distorted 0.41 Å above the equatorial plane formed by the three equatorial N donors toward the Br^-.

$[Ni(L^{Me})Cl]BPh_4$ was crystallized by slow diffusing of diethyl ether into a concentrated CH_3CN solution. The molecular structure of $[Ni(L^{Me})Cl]^+$ is shown in Figure 3B and related bond lengths and angles are listed in Table 2. The Ni center in $[Ni(L^{Me})Cl]^+$ is positioned in a distorted TBP coordination geometry (τ_5 = 0.86). The average Ni-Neq (2.110(3) Å) and Ni-Cl (2.267(1) Å) bond lengths in $[Ni(L^{Me})Cl]^+$, are slightly shorter (ca. 0.02-0.03 Å) than the corresponding bond lengths in $[Ni(Me_6tren)Cl]+$ complexes.[47,48] The Ni^{II} center in $[Ni(L^{Me})Cl]^+$ is distorted 0.29 Å out of the equatorial plane toward Cl^-.

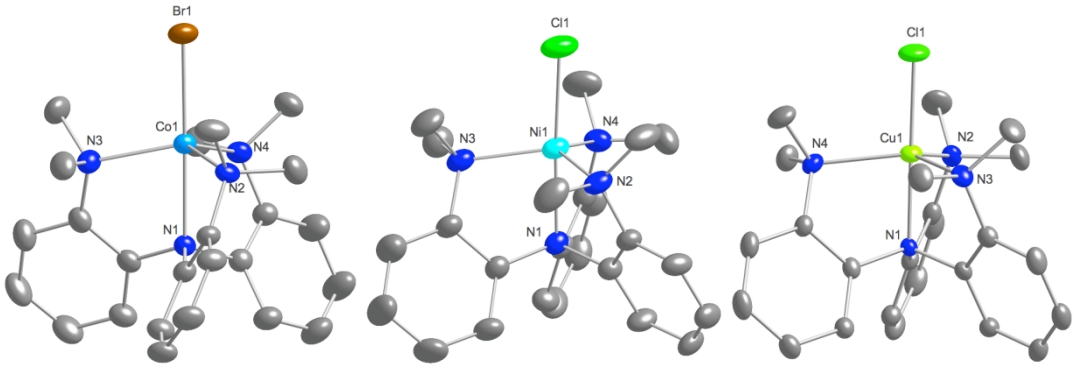

Figure 3. Molecular structures of $[Co(L^{Me})Br]^+$, $[Ni(L^{Me})Cl]^+$ and $[Cu(L^{Me})Cl]^+$ drawn at 30% probablility. Hydrogen atoms and counter aions have been removed for clarity.

The $[Cu(L^{Me})Cl]BF_4$ was crystallized as light yellow-green blocks from an CH_3CN/Et_2O solution. The Cu^{II} lies in a slightly distorted TBP coordination environment (τ_5 = 0.97) and is distorted 0.26 Å out of the equatorial plane. The bond lengths and angles are close to those observed in the related $[Cu(Me_6tren)Cl]^+$ species (τ_5 = 1.0).[9, 25] For instance, the average Cu-N_{eq} bond length in $[Cu(L^{Me})Cl]^+$ is 2.144(3) Å, compared to 2.186(2) Å in [Cu(Me_6tren)Cl]+.

Table 2. Selected bond lengths (Å) and angles (°) for $[Co(L^{Me})Br]BPh_4$, $[Ni(L^{Me})Cl]BPh_4$, and $[Cu(L^{Me})Cl]BF_4$.

	$[Co(L^{Me})Br]^+$	$[Ni(L^{Me})Cl]^+$	$[Cu(L^{Me})Cl]^+$
M1-X1	2.4167(4)	2.2667(13)	2.2121(8)
M1-N1	2.2280(18)	2.114(3)	2.0512(18)
M1-N2	2.1348(19)	2.135(3)	2.131(3)
M1-N3	2.1339(19)	2.080(3)	2.140(3)
M1-N4	2.123(2)	2.114(3)	2.160(3)
N1-M1-X1	178.22(5)	177.26(10)	179.45(11)
N2-M1-X1	100.07(5)	97.56(10)	96.88(7)
N3-M1-X1	100.63(5)	100.05(10)	96.45(8)
N4-M1-X1	102.54(5)	96.62(10)	97.45(8)
N1-M1-N2	78.90(7)	81.32(13)	83.10(9)
N1-M1-N3	78.67(7)	82.69(13)	83.10(10)
N1-M1-N4	79.24(7)	82.10(13)	83.05(11)
N2-M1-N3	117.97(8)	115.33(14)	121.48(10)
N3-M1-N4	115.53(8)	113.09(14)	118.34(10)
N2-M1-N4	115.71(7)	125.81(14)	115.89(10)

The preceding X-ray diffraction studies demonstrate that L^{Me} ligand can be used to stabilize five-coordinate metal complexes with TBP coordination geometries. These complexes have solid-state molecular structures similar to those observed in complexes supported by the closely related Me_6tren ligand. An important difference between the two scaffolds is that the L^{Me} ligand scaffold gives rise to Fe^{II}, Ni^{II}, and Cu^{II} complexes that display more distorted five-coordinate geometries. The distortions are probably due to the more rigid aryl backbone of the L^{Me} ligand. For each pair of complexes described above, the average N_{eq}-M^{II}-N_{ax} bond angle in the $[M(L^{Me})X]^+$ complex was about 2° smaller than that in the $[M_{II}(Me_6tren)X]^+$ species.

I.IV Spectroscopic and Magnetic Properties of $[M^{II}(L^{Me})X]^+$ Complexes

All complexes in this work were characterized by infrared, UV-Vis, and ^{1}H NMR spectroscopy. The infrared spectra for the ligand exhibits a medium C-N stretching band at 1314 cm^{-1} that shifts to lower frequencies (1300 – 1255 cm^{-1}) upon metal ion coordination. The $[Fe(L^{Me})Cl]BPh_4$ complex is colorless in solution and gives rise to a paramagnetic ^{1}H NMR spectrum and a solution magnetic moment of μ_{eff} = 5.02 μ_B (CD_3CN, 298 K) that is consistent with a high-spin, S = 2 ground state. The $[Co(L^{Me})Br]BPh_4$ species is violet in solution and exhibits three absorption bands in UV-Vis absorption spectrum and a solution-state magnetic moment of 4.68 μ_B (CD_3CN, 298 K). These data are consistent with an S = 3/2 ground state. The green $[Ni(L^{Me})Cl]BPh_4$ complex is high spin with a S = 1 ground state (μ_{eff} = 3.47 μ_B) in solution (CD_3CN, 298 K). The magnetic and electronic

absorption data for $[Fe(L^{Me})Cl]BPh_4$, $[Co(L^{Me})Br]BPh_4$, and $[Ni(L^{Me})Cl]BPh_4$ suggest that TBP geometry observed in their solid-state structures is being maintained in solution.

The electronic spectrum of the $[Cu(L^{Me})Cl]BF_4$ exhibits two d-d absorption bands at 782 nm and 1033 nm with molar extinction coefficient of 146 and 306 $M^{-1}cm^{-1}$. This pattern of one low-energy absorbance accompanied by a higher energy, low intensity shoulder indicates that TBP Cu^{II} coordination geometry is being maintained in solution state.[15, 27, 49] Since $[Cu(L^{Me})Cl]^+$, $[Cu(Me_6tren)Cl]^+$,[9, 25] and the related $[Cu(tmpa)Cl]^+$ [15, 27] complexes all display almost perfect TBP coordination geometries (solid state τ_5 values of 0.97, 1.0, and 1.0) and solution-state electronic absorption spectra consistent with this geometry being maintained, it is possible to compare the absorption maxima of these complexes to determine a relative ligand field strength for this series of ligands.[5] In Table 3, the d-d transitions of this series of complexes are listed and suggest that the ligand field strength is Me_6tren (932 nm) > tmpa (955 nm) > L^{Me}(1033 nm).

Table 3. Electronic spectra data for $[Cu(Me_6tren)Cl]^+$, $[Cu(tmpa)Cl]^+$, and $[Cu(L^{Me})Cl]^+$ in CH_3CN.

	λ_{max}, nm (ε, M^{-1} cm^{-1})
$[Cu(Me_6tren)Cl]^+$	740 (187), 932 (440)[a]
$[Cu(tmpa)Cl]^+$	632 (90), 962 (210)[b]
$[Cu(L^{Me})Cl]^+$	782 (146), 1033 (306)[c]

[a] ref.5, [b] ref 15, [c] this work

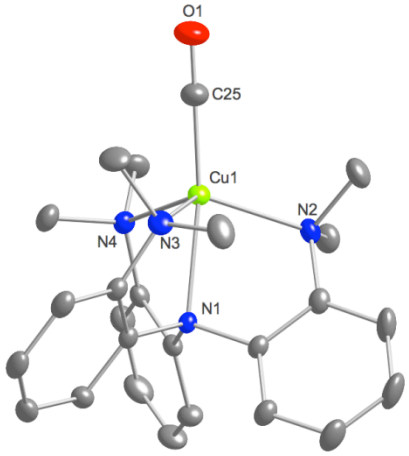

Figure 4. Molecular structure of $[Cu(L^{Me})CO]^+$ drawn at 30% probility. The anion (PF6-) and H atoms have been removed for clarity. Selected bond lengths (Å) and angles (°): average Cu-N_{eq} 2.24, Cu-N_{ax} 2.347(2), Cu-C 1.838(3), C-O 1.124(4).

Part V. Cu(I) Carbonyl Complexes

To investigate nucleophility of chelating ligands, it is instructive to compare the CO stretching frequencies (ν_{CO}) for the corresponding Cu(I)-CO complexes. This approach has been used in a number of studies involving Cu(I) complexes.[11, 12, 29, 33, 50] In addition to providing information about necleophility of the multidentate ligands, Karlin and co-workers have also used the infrared spectra of Cu(I)-CO complexes to provide information about the solution-state equilibira.[12, 29, 51] For example, they have demonstrated that all three pyridine donors are coordinated in the solid-state molecular structures of $[Cu(tmpa)CO]^+$.[12] This five-coordinate complex gives rise to a single ν_{CO} at 2077 cm^{-1} (nujol). In solution, the CO stretching frequency shifts to 2090 cm^{-1} in THF and 2092 cm^{-1} in

CH_3CN. The shift to higher frequency upon dissolution is attributed to a change in coordination number of Cu(I) center. Specifically, they have suggested that in solution equilibrium between the five-coordinate species in solid-state and a four-coordinate species in which one of the ligand arms is dissociated.[11, 12] To understand both the nucleophility of L^{Me} and solution state behavior of the complexes. We synthesized $[Cu(L^{Me})CO]^+$ by bubbling excess CO through an anhydrous acetone solution of $[Cu(L^{Me})]PF_6$. X-ray quality crystals were obtained by slow diffusing diethyl ether into a concentrated dichloromethane solution. The molecular structure of $[Cu(L^{Me})CO]PF_6$ is shown in Figure 4. The Cu(I) center displays a distorted TBP coordination geometry with average Cu-N_{eq} bond length of 2.24 Å and Cu-N_{ax} bond length of 2.347(2) Å. All of the Cu-N bond lengths are quite long for Cu(I)-NR_3 bond lengths.[52] For completeness, the Cu(I)-CO complex of the Me_6tren ligand scaffold has also been prepared and its infrared spectroscopy analyzed. Unfortunately, this complex has yet to isolated as crystals suitable for X-ray crystallography.

The ν_{CO} values for $[Cu(Me_6tren)CO]^+$, $[Cu(tmpa)CO]^+$, and $[Cu(L^{Me})CO]^+$ are shown in Table 4. Both $[Cu(tmpa)CO]^+$ and $[Cu(L^{Me})CO]^+$ exhibit their lowest ν_{CO} values (2077 cm^{-1} and 2088 cm^{-1}) in nujol where both complexes are five-coordiante.[11, 12, 33] When $[Cu(tmpa)CO]^+$ and $[Cu(L^{Me})CO]^+$ are dissolved in THF, their ν_{CO} values shift to slightly higher frequencies (2090 cm^{-1} and 2094 cm^{-1}) consistant with the presence of four-coordinate complex in solution. In the case of $[Cu(L^{Me})CO]^+$, two distinct ν_{CO} bands (2096 cm^{-1} and 2069 cm^{-1}) are observed when its spectrum is recorded in CH_3CN. We postulate that these two bands correspond to the existence of two distinct isomers

(four-coordinate and five-coordinate, respectively) in solution (Figure 5). This type of solution-state isomerism has been observed on $[Cu(TMPA^{R})CO]^{+}$ (R = OMe or NMe_2) complexes with electron donating substituent.

Table 4. Infrared stretching frequencies for Cu(I)-carbonyl complexes.

	$\nu_{CO}(cm^{-1})$ nujol	$\nu_{CO}(cm^{-1})$ THF	$\nu_{CO}(cm^{-1})$ CH_3CN
$[Cu(Me_6tren)CO]^{+}$	2098	2078	2085
$[Cu(tmpa)CO]^{+}$	2077	2090	2092
$[Cu(L^{Me})CO]^{+}$	2088	2094	2069, 2096

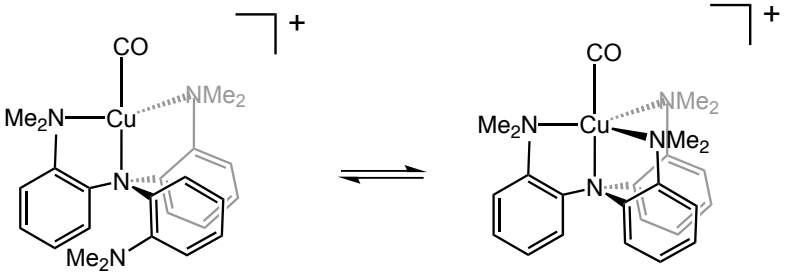

Figure 5. Five and four-coordinate isomers of $[Cu(LMe)(CO)]^{+}$

The ν_{CO} values for [Cu(Me_6tren)CO]+ have also been recorded as a nujol mull and in THF and CH_3CN solutions (Table 4). The trend observed for this complex is different. Specifically, [Cu(Me_6tren)CO]$^+$ exhibits highest ν_{CO} value in nujol. Based on the ν_{CO} values reported for other four-coordinate Cu(I)-CO complexes supported by three neutral N donor ligands,[12, 53, 54] we hypothesize that in the solid state, [Cu(Me_6tren)CO]$^+$ exist exclusively as four-coordinate complex with Me_6tren ligand coordinate in a κ^3 fashion. The κ^3 coordination mode of Me_6tren has been observed before in the solid-state molecular structure of square-planar Pd complex.[55] In THF and CH_3CN solutions, the ν_{CO} of [Cu(Me_6tren)CO]$^+$ shifts to lower frequencies suggesting the coordination of solvent molecules. Varied low temperature NMR (-10, -30, -50, -70, -90 °C, CD_3OD) always showed six kinds of H which confirm the κ^3 coordination mode of Me_6tren. The solution-state ν_{CO} data for [Cu(Me_6tren)CO]$^+$, [Cu(tmpa)Cl]$^+$, and [Cu(L^{Me})CO]$^+$ allow us to order this series of ligands in term of their nucleophility. The relative order, Me_6tren > tmpa > L^{Me}, is reasonable based on the pKa values of the conjugate acids of the ligand donor groups (i.e., [*N,N*-dimethylethylammonium]$^+$ (0.83 ± 0.28); [2-methylpyridinium]$^+$ (5.95 ± 0.28); and [*N,N*-dimethylbenzylammonium]+ (5.1 ± 0.28)).[56]

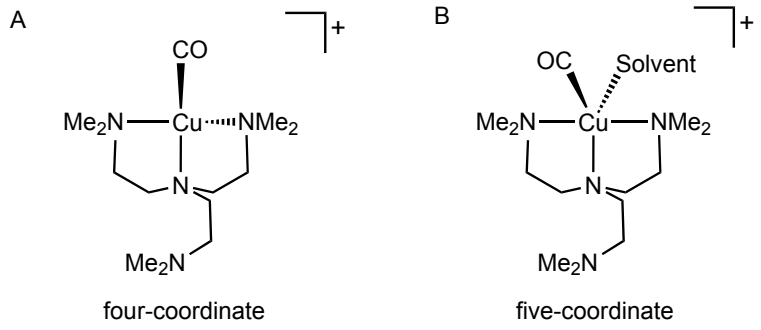

Figure 6. Equilibrium of $[Cu(Me_6tren)(CO)]^+$ in solution state

Part VI. Conclusions

A new neutral tetradentate tetraamine ligand, L^{Me}, that incorpates N,N'-dimethylaniline donor groups into a tripodal framework has been synthesized. A series of M^{II}-halide complexes, $[M^{II}(L^{Me})X]^+$, have been synthesized and their solution-state and solid-state structures evaluated. The rigid aryl backbone of L^{Me} gives rise to M(II)-halide complexes with distorted TBP structures. Electronic absorption and infrared spectroscopy studies confirm that L^{Me} is a weaker-field ligand with less nucleophility than both TMPA and Me6tren. Comparative infrared studies on the Cu(I)-CO complexes $[Cu(L^{Me})CO]^+$ and $[Cu(Me_6tren)CO]^+$ illustrates that in some cases these ligands can display very different coordination topologies. We believe the weak-field electronic characteristics and inherent rigidity of L^{Me} ligand may help creat transition metal fragments that exhibit distinct reactivity.

Part II. Chemistry of Cu(I)-O_2 Complexes supported by L^{Me}

Part II.I Cu-O Derived Species and Biological Functions

Cu-O derived species are active centers in many kinds of metalloprotein enzymes, and some Cu complexes with tripodal tetraamine ligands have been proved to be good small molecule models for these systems. A dicopper(II)-μ-η^2:η^2-peroxo is the structure (**Figure 7)** formed in hemocyanin (Hc) which is the O_2-carrier for anthropods and mollusks.[57] Mononuclear copper(II)-superoxide (Cu^{II}-O_2^-) or copper(II)-hydroperoxide (Cu^{II}-OOH) species (**Figure 8**) are believed to be the active center of dopamine β-monooxygenase (DβM) and peptidylglycine α-amidating monooxygenase (PHM) which catalyze aliphatic C-H bond hydroxylation.[58] Two active-site Cu ions are separated by about 11 Å which is too far to accommodate a bridging dioxygen derived species (**Figure 9**).[59]

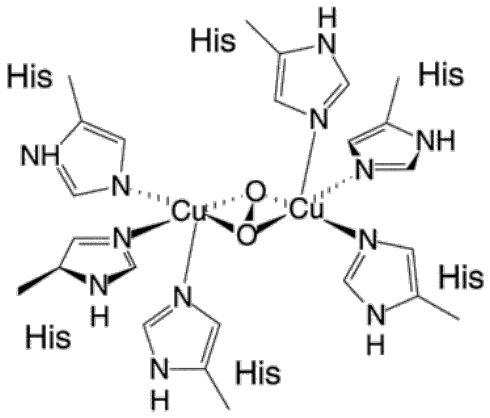

Figure 7. Dioxygen-binding mode as found in the HC crystal structure.[57]

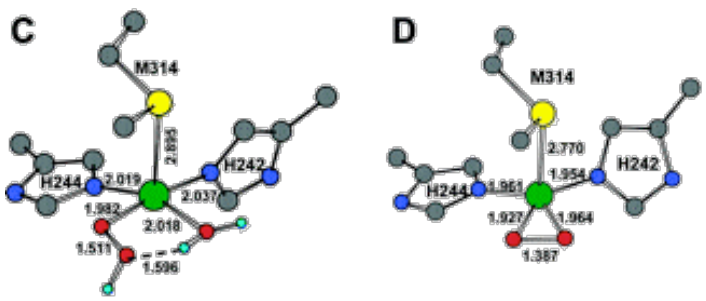

Figure 8. Energy optimized structures: (C) Cu^{II}-OOH. (D) Cu^{II}-$O_2^{\cdot-}$.[58]

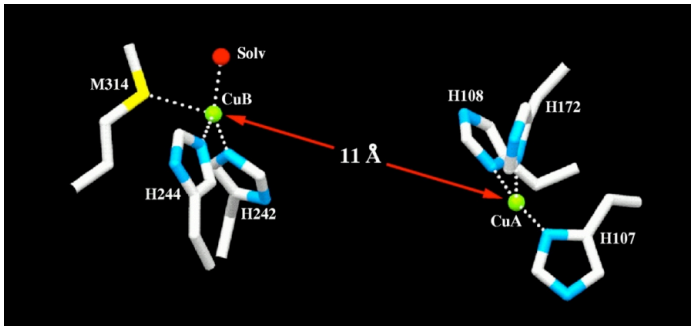

Figure 9. Coordination geometry of CuA and CuB.[59]

Part II.II Cu-O Complexes for Aliphatic C-H Activation

Biomimetic studies are very useful in the development of chemistry involving Cu(I)-O_2 interactions by elucidating the nature of possible Cu_n-O_2 (n =1, 2) species and their reactivity mechanisms. Generally, tetradentate tripodal tetraamine ligands give the end-on μ-1, 2-peroxo coordination mode, while tridentate or bidentate N-donor ligands yield side-on μ-η^2:η^2-peroxo-dicopper(II) complexes or related bis-μ-oxo-dicopper(III) species

and they are usually in rapid equilibrium (**Scheme 3**).[60] Other well-characterized copper complexes with O-O bonds include mono- or dicopper(II) species with a superoxo (O_2^-) or hydroperoxo(HOO^-) moiety. All possible binuclear and mononuclear Cu-O_2 species are listed (**Chart 2).**

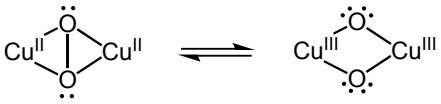

Scheme 3. Equilibrium between $[\{Cu^{II}L\}_2(\mu\text{-}\eta^2\text{:}\eta^2\text{-}O_2^{2-})]^{2+}$ and$[\{Cu^{II}L\}_2(\mu\text{-}1, 2\text{-}O_2^{2-})]^{2+}$

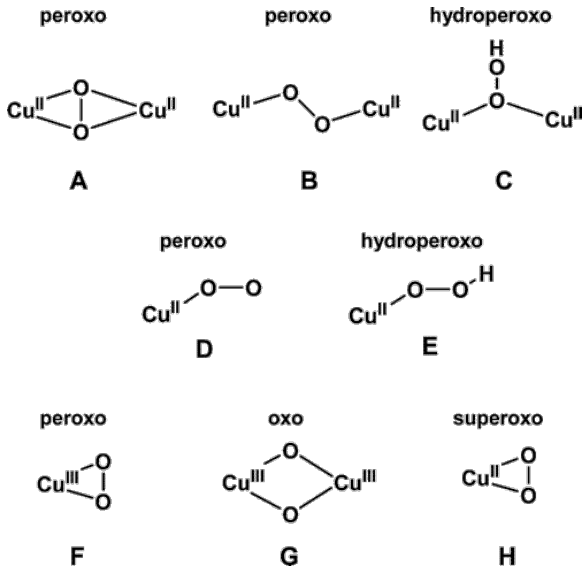

Chart 2. Possible binuclear and mononuclear Cu-O_2 species

Binuclear Cu-O_2 derived species have been demonstrated to initiate aliphatic C-H bond oxidations. Recent advances in Cu-O chemistry of synthetic complexes have shown that ligand character (chelate ring size, donor type, substituent on or near donors), counter ion and solvent dramatically influences Cu_2O_2 structures and reactivity. Itoh and co-workers have reported a dicopper(III)-bis-μ-oxo $\{Cu^{III}_2\text{-}(O^{2-})_2\}$ complex, stabilized by pyridylalkylamine ligands, that effects an internal (ligand-based) benzylic hydroxylation reaction.[61] Tolman and co-workers discovered intramolecular ligand oxidative *N*-dealkylation chemistry with $Cu^{III}_2\text{-}(O^{2-})_2$ species that consist of alkyl-substituted triazacyclononane ligands.[62] Karlin and co-workers described the$\mu\text{-}\eta^2\text{:}\eta^2$-peroxo-dicopper(II)/ bis-μ-oxo-dicopper(III) oxidative *N*-dealkylation of exogenous substrate *N,N*-dimethylanilines and THF 2-position hydroxylation.[63,64] Suzuki and co-workers have alos reported a dicopper(II)-μ-hydroxo-μ-hydroperoxo entity that effects intramolecular methylene hydroxylation of a coordinated ligand (an $ArCH_2NR_2$ group) and subsequent N-dealkylation.[65] This section describes the reactivity of $[Cu^I(L^{Me})]^+$ with dioxygen and the ability to effect catalytic intermolecular C-H bond activation.

Part II.III Results and Discussion

Synthesis and Stability of the Blue Powder

The white powder $[Cu(L^{Me})]PF_6$ reacts with pure, dry O_2 in anhydrous acetone at room temperature to form intense blue precipitate. This blue species is only soluble in

coordinating solvents. Upon dissolution in coordinating solvents, it initially forms an intense blue solution; but this solution decays within several minutes to afford a light green solution. The blue product can be dispersed in non-coordinating solvent such as CH_2Cl_2, benzene, toluene to form relative stable, heterogeneous mixtures at room temperature. Unfortunately, the blue species could not be crystallized to produce X-ray quality crystals. However, the green product formed by dissolving the blue species in acetone was readily recrystallized by the diffusion of Et_2O into a concentrated solution of the green product. X-ray crystallography confirmed the green product to be $[Cu^{II}(L^{Me})(OH)]PF_6$ (**Figure 10).** These results may represent the first X-ray crystallographically characterized, mononuclear decay product of a Cu-dioxygen intermediate.

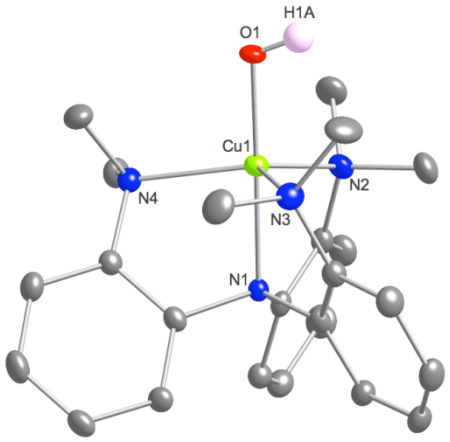

Figure 10. Molecular structure of $[Cu(L^{Me})(OH)]^+$

Based on the structure of decay product, we predict the blue intermediate to be

$[\{Cu^{II}(L^{Me})\}_2(\mu\text{-}1,2\text{-}O_2^{2-})](PF_6)_2$ which is similar to the $[\{Cu^{II}(Me_6tren)\}_2(\mu\text{-}1,2\text{-}O_2^{2-})](BPh_4)_2$ complex discovered by Schindler and co-workers.[66] Both complexes have intense blue powdery appearance and extraordinary stability at room temperature. Unlike other reactive Cu-dioxygen complexes (e.g., $[\{Cu^{II}(Me_6tren)\}_2(O_2)](ClO_4)_2$, $[\{Cu^{II}(Bz_3tren)\}_2(O_2)](BPh_4)_2$ and $[\{Cu^{II}(tmpa)\}_2(O_2)](PF_6)_2$), which must be handled at very low temperature[67] (ca. -80 °C), $[\{Cu^{II}(L^{Me})\}_2(\mu\text{-}1,2\text{-}O_2^{2-})](PF_6)_2$ incredible stability suggests the dioxygen intermediate is stable and does not undergo reversible dissociation of the coordinated dioxygen ligand.[68] In Schindler's work, the special crystal packing structure affords for the extraordinary stability of $[\{Cu^{II}(Me_6tren)\}_2(O_2)](BPh_4)_2$ at room temperature. The copper containing cation is completely shielded by eight BPh_4^- anions, and this encapsulation suppresses any further reactions (**Figure 11**).[66] The related stability of $[\{Cu^{II}(L^{Me})\}(O_2)](PF_6)_2$ is probably due to the same effect, that is shielding of the copper cation in the solid state by the PF_6^- anions. The time-resolved UV-Vis spectra of reaction of $[Cu(L^{Me})](PF_6)$ and O_2 in a coordinating solvent (CH_3CN) was recorded (**Figure 12**). It shows the decay of the postulated $[\{Cu^{II}(L^{Me})\}_2(\mu\text{-}1,2\text{-}O_2^{2-})](PF_6)_2$ species to the $[Cu^{II}(L^{Me})(OH)]PF_6$ complex. Labeling studies ($^{18}O_2$) need to be preformed in the future to determine the source of the oxygen in the coordinating hydroxo unit.

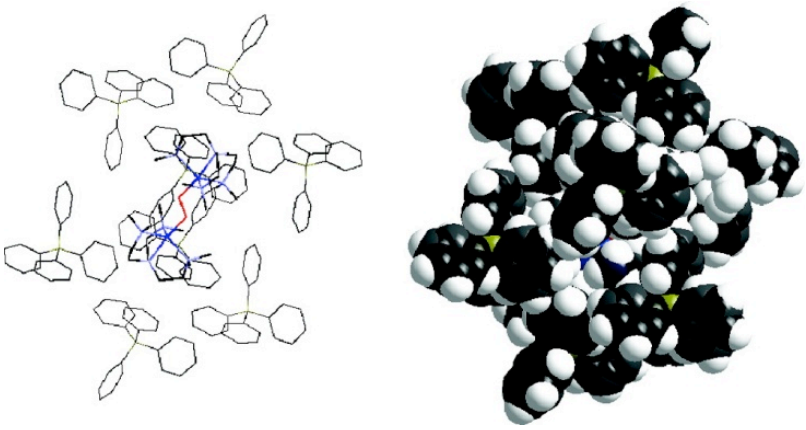

Figure 11. Aion shielding in $[\{Cu^{II}(Me_6tren)\}_2(O_2)](BPh_4)_2$

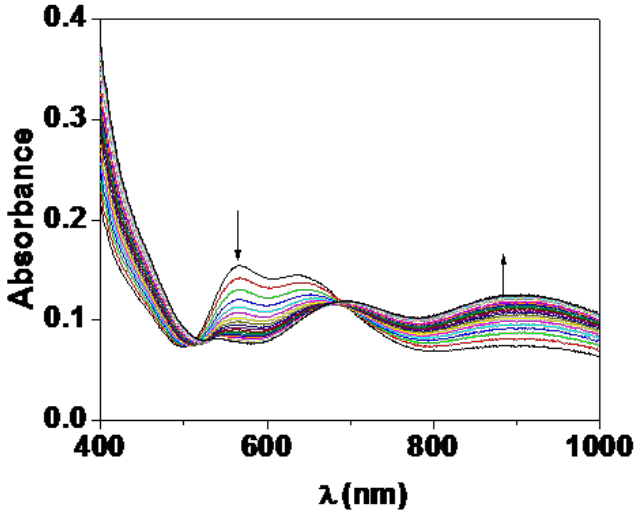

Figure 12. Reaction of $[Cu(L^{Me})]PF_6$ with O_2 at 10 °C in normal CH_3CN ([complex] = 1 mM, Δt = 12 s, total time is 120 s)

Part II.IV C-H Activation of Toluene

A mixture of 25 mg of the blue powder and 2 ml anhydrous toluene was sparged with dry O_2 for 30 min and then stirred at 60 °C for seven days. There was basically no color change and GC analysis only showed very little conversion of toluene to $PhCH_2OH$ and PhCHO. The extremely low reactivity exhibited by the blue powder under these conditions is probably caused by the very low solubility of this species in toluene. In order to improve its solubility in non-polar solvents, the large organic anion BPh_4^- was exchanged for the PF_6^- anion in the blue Cu-peroxo complex. However, the direct oxidation of $[Cu(L^{Me})]BPh_4$ by O_2 does not form stable "blue" complexes in common organic solvents either at room temperature or low temperatures (-80 ºC). It is believed that counter-ions, solvents and temperature play import roles in the reactivity of Cu-peroxo complexes from the summary of decades work.

If a mixture of dioxgyen saturated anhydrous toluene, the Cu-oxygen containing blue powder, and two equivalents of $NaBPh_4$ are sealed in a Schlenk flask and stirred overnight at room temperature a yellow-brown solution results. GC analysis of the reaction mixture showed the selective formation of PhCHO over $PhCH_2OH$ (about 40:1 selectivity by GC). This oxidation reaction is most likely catalyzed by the in-situ formation of Cu-peroxo complex with BPh_4^- counter-ion. This great difference in reactivity confirms the importance of solubility of the Cu-peroxo complex.

Part II.V Possible Mechanisms

The responsible reactive species in the C-H oxidation of toluene may be a mononuclear Cu^{II}-superoxide complex $[LCu^{II}(O_2^{\cdot-})]^+$. It can be formed by either oxygenation of $[LCu^{I}]^+$ or dissociation of $[(LCu^{II})_2(O_2^{\cdot-})]^{2+}$. The research of Karlin and co-workers shows that weaker field ligands favor the formation of Cu-superoxo complexes with stronger O-O bond. From the discussion in Part I, L^{Me} is confirmed to be weaker field ligand than Me_6tren and TMPA, so $[(L^{Me}Cu^{II})_2(O_2^{2-})]^{2+}$ should have stronger O-O bond which can remain in Cu^{II}-superoxide intermediate $[L^{Me}Cu^{II}(O_2^{\cdot-})]^+$. The Cu^{II}-superoxide species $[LCu^{II}(O_2^{\cdot-})]^+$ is the actual hydrogen atom abstractor of toluene. The resulting copper-hydroperoxide $[LCu^{II}(HOO^{-})]^+$ moiety could further react with the benzyl radical by a formal HOO• rebound reaction, releasing $[LCu^{I}]^+$ and benzylhydroperoxide product; the latter could eliminate water to give benzaldehyde (Scheme 4).[76] Benzyl radical may also react with the excess O_2 dissolved in the solvent to form benzylperoxyl radical. Reduction of the benzylperoxyl radical ($PhCH_2OO$•) by $[LCu^{I}]^+$ present in the system could generate $[LCu^{II}\text{-}OOCH_2Ph]^+$ followed by elimination of $[LCu^{II}OH]^+$ and PhCHO generation (Scheme 5).[77]

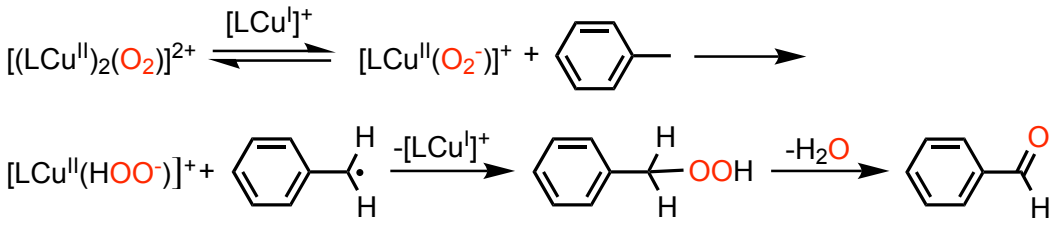

Scheme 4. Pathway of the C-H oxidation by Cu-peroxo complex

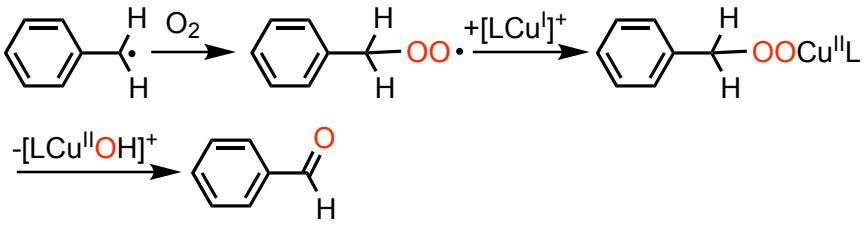

Scheme 5. Another possible pathway of C-H oxidation

Part II.VI Conclusions

The new tripodal tetradentate tetraamine ligand L^{Me} can support a dinuclear Cu^{II}-peroxo complex (the blue powder, possibly $[(L^{Me}Cu)_2(O_2^{2-})]^{2+}$) that exhibits extraordinary stability at room temperature. The most striking characteristic of the blue powder is the selective aliphatic C-H bond oxidative ability. Initial catalytic investigations demonstrate that the $[(L^{Me}Cu)_2(O_2^{2-})]^{2+}$ can catalyze the selective oxidation of toluene and affords product selectivity of ~ 40:1 (PhCHO to $PhCH_2OH$). The essential part of possible mechanism is the generation of benzyl radical by the oxidation of mononuclear Cu^{II}-superoxo complex. The ligand field imparted by L^{Me} and its rigid coordination abilities are key to achieving selectivity in these oxidation reactions.

Part III. Experimental Section

All reactions were performed using standard Schlenk techniques in an MBraun Labmaster 130 drybox under an atmosphere of dinitrogen unless otherwise stated. All reagents were all obtained from commercial chemical vendors and were used without further purifications unless otherwise noted. Anhydrous solvents were purchased from Sigma-Aldrich and further purified by sparging with Ar gas and passage over activated

alumina columns. Elemental analyses were performed by Columbia Analytical Services, Tucson, AZ or Atlantic Microlab, Inc., Norcross, GA. Ambient temperature ^{1}H NMR spectra were recorded on a Varian Mercury 300MHz spectrophotometer. Varies low temperature ^{1}H NMR spectra were recorded on a Varian Unity 600MHz spectrophotometer. Chemical shifts (δ) are reported in parts per million (ppm) and coupling constants (J) are reported in Hz. NMR spectra were referenced internally to residual solvent. IR spectra were recorded as KBr pellets on a Varian Scimitar 800 Series FT-IR spectrophotometer. Nujol and solution state IR spectra were recorded using the same spectrophotometer with KBr salt plates. UV-Visible absorption spectra were recorded on a Cary 50 spectrophotometer using 1.0 cm or 0.5 cm quartz cuvettes. Solution state magnetic moments were measured using the Evans' method.[57, 58] Mass spectra were recorded in the Mass Spectrometry Center at Emory University on a JEOL JMS-SX102/SX102/A/E mass spectrometer. X-ray crystallography studies were carried out in the X-ray Crystallography Laboratory at Emory University on a Bruker Smart 1000 CCD diffract meter. Cyclic voltammetric experiments were carried out using a CH Instruments (Austin, TX) Model 660C potentiostat using a three-component cell consisting of a Pt auxiliary electrode, a non-aqueous reference electrode ($Ag/AgNO_3$), and a platinum working electrode (3 mm). All electrochemistry experiments were conducted in CH_3CN or DMF with 0.10 M $[N(t\text{-}Bu)_4]PF_6$ as the supporting electrolyte. All electrochemical measurements are referenced and reported versus the Fc/Fc^+ couple. The ligands Tren, $N(o\text{-}PhNH_2)_3$,[41, 59] and Me_6tren[16] and $[Cu(Me_6tren)]PF_6$[10] were synthesized using published literature methods.

Tris(2-dimethylaminophenyl)amine, (L^{Me}). An aqueous HCHO solution (37 w.%) (6.61 ml, 88.0 mmol) was added to an CH_3CN (100 ml) solution of $N(o\text{-}PhNH_2)_3$ (0.7993 g, 2.75 mmol) and stirred. After 30 minutes, powdery $NaBH_3CN$ (1.6510 g, 26.3 mmol) was added to the solution. Once all of the NaBH3CN was dissolved, concentrated HOAc (0.6 ml) was added drop-wise to adjust the pH to ~ 7 and the reaction mixture was stirred for 12 hrs. All volatiles were then removed under reduced pressure to yield a sticky, off-white solid. A KOH solution (2 M, 50 ml) was added to the crude solid and Et_2O (3 x 20 ml) was used to extract the product. The organic layer were combined and washed with KOH solution (0.5 M, 50 ml). The organic layer was then extracted with an aqueous HCl solution (1 M, 3 x 15 ml). The aqueous extracts were combined and neutralized using solid KOH. The product was then extracted using Et_2O (3 x 20 ml). The Et_2O washes were combined and dried over K_2CO_3. The filtrate was concentrated to dryness using a rotary evaporator to yield a light pink solid. The light pink solid was recrystallized from hot methanol to yield the product as off-white needles (77%, 0.7959 g). ^{1}H NMR ($CDCl_3$): 7.05 (dd, 3H, J=1.8, J=7.5), 6.98 (td, 3H, J=1.8, J=6.9), 6.86 (td, 3H, J=1.8, J=7.8), 6.78 (dd, 3H, J=1.8, J=7.8), 2.39 (s, 18H). HRMS (ESI): $C_{24}H_{30}N_4$ m/z Calcd. 374.24705 Found 375.25461 $[M+1]^+$. FTIR (KBr) $\tilde{\upsilon}_{max}$ (cm^{-1}): 3054, 2971, 2910, 2820, 2774, 1922, 1889, 1804, 1781; 1586, 1491, 1448, 1314, 1258, 954, 753.

Preparation of $[HL^{Me}]PF_6$. Off-white crystalline solid L^{Me} (0.0749 g, 0.2000 mmol) was

dissolved in 10 ml CH_3CN at room temperate. An aqueous solution of HPF_6 (~65 wt. % in water, 0.0253 ml, 0.1860 mmol) was added drop-wise to this solution. The reaction was stirred for 1h. All solvents was removed from the reaction mixture using a rotary evaportator to yield a white powder. The white powder was washed with Et_2O (3 x 10 ml) on a medium porosity frit to form fine white powder (0.0937 g, 0.1800 mmol, 97%). Micro scale colorless long needle X-ray quality single crystal can be obtained by diffusing Et_2O into THF solution of the product. ^{1}H NMR (CD3CN): 7.94 (br), 7.72 (br), 7.60 (t), 7.02 (br), 3.48 (br, N-H), 2.54 (br, NH-CH_3), 2.42(br, N-CH_3). FTIR (KBr) $\tilde{\upsilon}_{max}$ (cm^{-1}): 3139; 2991, 2851, 2741, 2685, 2538, 2427, 1490, 1448, 843. EM-MS (ESI): $[HL^{Me}]^+$ m/z Calcd. 375.25478. Found 375.25461.

Preparation of [Fe(Me_6tren)Cl]BPh_4. To a slurry of $FeCl_2$ (0.0715g, 0.5641mmol) in CH_2Cl_2 (10.0 ml) was added a solution of Me_6tren (0.1298g, 0.5634mmol) in 10ml CH_2Cl_2. After stirring 30min, $NaBPh_4$ (0.1936g, 0.5658mmol) was added drop-wise as a CH_3OH solution (2 ml) and the reaction stirred for an additional 3 h. During this time, a large amount of white precipitated had formed. The precipitate was isolated on a medium porosity frit and washed with CH_2Cl_2 (2 x 2 ml). The filtrate and CH_2Cl_2 washing were combined and concentrated to dryness to afford a white solid. Single crystals suitable for X-ray diffraction studies can be obtained by slow diffusion of Et_2O into DMF solution of the complex. FTIR (KBr) $\tilde{\upsilon}_{max}$ (cm^{-1}): 1950, 1886, 1825, 1764; 1579; ν (NMe_2) 1475, 1427;

736, 707. HRMS (ESI): $[Fe(Me_6tren)Cl]^+$ m/z Calcd. 321.15084. Found 321.15049 (100.00). Anal. Calcd (Found) for $[Fe(Me_6tren)Cl]BPh_4$: C, 67.46 (67.03); H, 7.86 (7.84); N, 8.74 (9.40).

Preparation of $[Fe(L^{Me})Cl]BPh_4$. To a suspension of $FeCl_2$ (0.0390g, 0.3077mmol) in 10.0 ml of CH_2Cl_2 was added a solution of L^{Me} (0.1194g, 0.3205mmol) in 10.0 ml of CH_2Cl_2 drop-wise. A solution of $NaBPh_4$ (0.1084 g, 0.3168 mmol) in CH_3OH (5 ml) was added drop-wise to the reaction mixture and precipitate formed immediately. The reaction mixture was stirred over 4h and the white precipitate was removed by filtering the reaction mixture through a medium porosity frit. Colorless block crystals suited for X-ray crystallography were grown by diffusing Et_2O into the CH_3CN solution of crude product. FTIR (KBr) $\tilde{\upsilon}_{max}$ (cm^{-1}): 3052, 2984, 2832, 2789, 1943, 1884, 1813, 1752, 1579, 1489, 1447, 1296, 1265, 1243, 734, 705. ^1H NMR (CD_3CN): 16.60(br), 13.60(br), 13.53(br), 10.67(br), 7.23(s), 6.97(t), 6.82(s). HRMS (ESI): $[Fe(L^{Me})Cl]^+$ m/z Calcd. 465.15084. Found 465.15053. Anal. Calcd (Found) for $[Fe(L^{Me})Cl]BPh_4$: C, 73.44 (73.31); H, 6.42 (6.63); N, 7.14 (7.05). μ_{eff} = 5.03 μ_B (Evans' Method, CD_3CN, 298 K).

Preparation of $[Co(L^{Me})Br]BPh_4$. To a stirred solution of L^{Me} (0.1862 g, 0.5 mmol) in 10.0 ml of CH_2Cl_2 was added $CoBr_2$ (0.1088 g, 0.5 mmol). The reaction was stirred for 30 minutes and then $NaBPh_4$ (0.1734 g, 0.5 mmol) was added drop-wise as a CH_3OH solution (2 ml). The reaction was refluxed under an atmosphere of N_2 for 3 hours. The reaction mixture was cooled to room temperature. All volatiles were removed under reduced pressure

to yield a purple precipitate. The precipitate was isolated on a medium porosity frit, washed with CH_3OH (10 ml), and dried under vacuum overnight (0.250 g, 60%). Single crystals for X-ray crystallography were formed by slow diffusion of Et_2O into CH_3CN solution of the product. Bulk recrystallization can also be used to isolate large quantities of analytical pure material by diffusion of Et_2O into THF solution of the product. ^{1}H NMR (CD_3CN): 19.45, 14.95 (br), 14.50 (br), 8.80 (br), 7.24 (s), 6.98(t), 6.80 (t). FTIR (KBr) $\tilde{\nu}_{max}$ (cm^{-1}): 3056, 3044, 2984, 1492, 1449, 1258, 1204, 1146, 1095, 1004, 921, 773, 731, 706, 611. UV-Vis (CH_3OH) λ_{max}, nm (ε, M^{-1} cm^{-1}): 510 (73), 534 (72), 620 (128). $\mu_{eff} = 4.68\mu_B$ (Evans' Method, CD_3CN, 298K). Anal. Calcd (found) for $[Co(L^{Me})Br]BPh_4$: C, 69.24 (68.99); H, 6.05 (6.13); N, 6.73 (6.75). HRMS (ESI): $[Co(L^{Me})Br]^+$ m/z Calcd. 512.09858 Found 514.09584 (100.00), 512.09786 (92.80).

Preparation of $[Ni(L^{Me})Br]BPh_4$. This complex was prepared in a manner similar with that of $[Co(L^{Me})Br]BPh_4$, except $Ni(PPh_3)_2Cl_2$ was used in place of $CoBr_2$. The product was isolated a light yellow-green powder (0.3560 g, 90%) and recrystallized for X-ray diffraction studies by the diffusion of Et_2O into a concentrated CH_3CN solution of the product.^{1}H NMR (CD_3CN): 23.54 (br), 16.48 (br), 14.80 (br), 7.22, 6.97 (t), 6.82 (t), 2.21 (br). FTIR (KBr) $\tilde{\nu}_{max}$ (cm^{-1}): 3054, 3031, 2983, 2928 1492, 1426, 1259, 1198, 1144, 1094, 1032, 1005, 772, 733, 705, 669, 613 585. UV-Vis (CH_3OH) λ_{max}, nm (ε, M^{-1} cm^{-1}): 440 (112), 684 (30). μ_{eff} = $3.47\mu_B$ (Evans Method, CD_3CN, 298K). Anal. Calcd (found) for $[Ni(L^{Me})Cl]BPh_4 \bullet 1/2THF$: C, 72.62 (73.17); H, 6.80 (6.52); N, 6.51 (6.77).

Preparation of $[Cu(L^{Me})Cl]BF_4$. A green CH_3OH solution (8 ml) of $CuCl_2$ (0.1338 g, 0.9952 mmol) was added to a stirring methanol solution (15ml) of L^{Me} (0.3728 g, 0.9954 mmol) resulting in the immediate formation of a dark red reaction mixture. The reaction was stirred at room temperature for 10 min. Colorless $AgBF_4$ (0.1942 g, 0.9976 mmol) was then added drop-wise as a CH_3OH solution (5 ml) to reaction mixture. The mixture was stirred overnight and filtered through a pad of celite to remove AgCl. The filtrate was concentrated using a rotary evaporator to yield a bright yellow solid. This solid was collected on a medium porosity frit and washed with a 10:1 Et_2O/CH_3CN solution (10 ml) to yield a yellow-green solid (0.49 g, 88%). Single crystals for X-ray crystallography were grown by diffusing Et_2O into saturated CH_3CN solution of crude product. ^1H NMR (CD_3CN): 18.20 (br), 13.55 (br), 12.00 (br), -4.4 (br). FTIR (KBr) $\tilde{\nu}_{max}$ (cm^{-1}): 3054, 3031, 2931, 2852, 2820, 2775, 1492, 1472, 1288, 1062, 1007, 922, 732, 587, 480. UV-Vis (CH_3CN) λ_{max}, nm (ε, $M^{-1}.cm^{-1}$): 430 (sh) (1025), 782 (146), 1033 (306). Anal. Calcd (Found) for $[Cu(L^{Me})Cl]BF_4$: C, 51.44 (51.73); H, 5.40 (5.44); N, 10.00 (10.18). HRMS (ESI): $[Cu(L^{Me})Cl]^+$ m/z Calcd. 475.14550. Found 472.14520 (100.00). μ_{eff} = 1.83 μ_B (Evans Method, $CDCl_3$, 298K).

Preparation of $[Cu(L^{Me})]PF_6$. To an CH_3CN solution (3.0 ml) of $[Cu(CH_3CN)_4]PF_6$ (0.0754 g, 0.2023 mmol) was added a solution of L^{Me} (0.0786 g, 0.2099 mmol) in CH_3CN (3 ml). The reaction was stirred at room temperature overnight. The solvent was removed under reduced pressure to afford a white powder. The powder was washed with Et_2O and dired on a sintered glass frit (0.1058 g, 0.1815 mmol, 89.7%). Colorless crystals can be grown

by diffusing Et_2O into CH_3CN solution but can't be solved by X-ray crystallography. ^1H NMR (CD3CN): 7.10 (3H), 7.00 (3H), 6.88 (3H), 6.70 (3H), 2.37 (18H). FTIR (KBr) $\tilde{\nu}_{max}$ (cm^{-1}): 3059, 2932, 2821, 2775, 1492, 1448, 1261, 1225, 1099, 1048, 841, 771, 558. MS (EM-ESI): $[Cu(L^{Me})]^+$ m/z Calcd. 437.17665. Found 437.17560(^{63}Cu, 100), 439.17413(^{65}Cu, 44.33).

Preparation of $[Cu(L^{Me})(CO)]PF_6$. Solid $[Cu(L^{Me})]PF_6$ (0.0512 g, 0.0878 mmol) was dissolved in dry acetone (10 ml) and transferred to a Schlenk flask. The colorless solution was then sparged with CO gas for 30 min. Over this time period, the reaction mixture changed from colorless to light green. The resulting solution was layered with Et_2O and allowed to stand overnight. Light green crystals of the product formed (0.0266 g, 49.5%). Crystals suitable for X-ray crystallography was grown by diffusing Et_2O into a CH_2Cl_2 solution of the complex. ^1H NMR (CD_3CN): 7.16(3H), 7.00(3H), 6.85(3H), 6.66(3H) 2.37(18H). FTIR (KBr) $\tilde{\nu}_{max}$ (cm^{-1}): 3072, 2884, 2813, (CO) 2088, 1493, 1449, 1271, 1218, 1101, 1051, 1019, 840, 768, 558. FTIR (THF) $\tilde{\nu}_{max}$ (cm^{-1}): (CO) 2094. FTIR (Nujol) $\tilde{\nu}_{max}$ (cm^{-1}): (CO) 2088.

Preparation of $[Cu(Me_6tren)(CO)]PF_6$. Under an inert atmosphere, a Schlenk tube was charged with Me_6tren (0.10 g, 0.44 mmol), 10.0 ml of THF, and a stir bar sealed with a septum. In a separate Schlenk tube, $[Cu(CH_3CN)_4]PF_6$ (0.16 g, 0.44 mmol) was dissolved in THF and fitted with a septum. Both solutions were then saturated with CO(g) by bubbling

each solution with CO(g) for 30 minutes. The Me6tren solution was transferred to the $[Cu(CH_3CN)_4]PF_6$ solution by cannual. The reaction mixture changed from colorless to pale green upon immediately. The reaction mixture was layered with Et_2O and allowed to stand overnight and produced a pale green microcrystalline powder. The solid was collected on a frit and washed with Et_2O (0.15 g, 88%). The pale green solid is very reactive toward O_2 and difficult to store as a solid or solution for long periods of time. FTIR (THF) $\tilde{\nu}_{max}$ (cm^{-1}): (CO) 2078. FTIR (Nujol) $\tilde{\nu}_{max}$ (cm^{-1}): (CO) 2098.

X-ray Diffraction Studies. Suitable crystals of $[HL^{Me}]PF_6$, $[Fe(Me_6tren)Cl]BPh_4$, $[Fe(L^{Me})Cl]BPh_4$, $[Co(L^{Me})Br]BPh_4$, $[Ni(L^{Me})Cl]BPh_4$, $[Cu(L^{Me})Cl]BF_4$, and $[Cu(L^{Me})(CO)]PF_6$, were coated with Paratone N oil, suspended in a small fiber loop and placed in a cool N_2 gas stream at 173 K on a Bruker D8 APEX II CCD sealed tube diffractometer with graphite monochromated MoKα (0.71073 Å) radiation. Data were measured using a series of combination of phi and omega scans with 10 s frame exposure and 0.5° frame widths. Data Collection, indexing and initial cell refinements were all carried out using APEX II[72] software. Frame integration and final cell refinements were done using SAINT[73] software. All structures were solved using direct methods and difference Fourier techniques (SHELXTL, V6.12).[74] Hydrogen atoms were placed on their expected chemical position using the HFIX command and were include in the final cycles of least squares with isotopic Uij's related to the atom's ridden upon. All non-hydrogen atoms were refined anisotropically except for the acetonitrile solvent molecules in $[Fe(Me_6tren)Cl]BPh_4$, $[Co(L^{Me})Br]BPh_4$, and

$[Ni(L^{Me})Cl]BPh_4$ and the disordered F atoms in $[Cu(L^{Me})(CO)]PF_6$. Scattering factors and anomalous dispersion corrections are taken from the International Tables for X-ray crystallography.[75] Structure solution, refinement, graphics and generation of publication materials were performed by using SHELXTL, V6.12 software. Additional details of data collection and structure refinement are given in Table 5. CCDC 766572 – 766578 contain the supplementary crystallographic data for this manuscript. These files can be obtained free of charge from the Cambridge Crystallographic Data Centre via http://www.ccdc.cam.uk/data request.cif.

Table 5. Crystal data and refinement data for $[HL^{Me}]PF_6$ and $[Fe(L^{Me})Cl]BPh_4$

	$[HL^{Me}]PF_6$	$[Fe(L^{Me})Cl]BPh_4$
Empirical Formula	$C_{24}H_{31}F_6N_4P$	$C_{48}H_{50}BClFeN_4$
Crystal system	Monoclinic	Monoclinic
Space Group	P2(1)/c	Pc
a, Å	7.792(5)	10.066(11)
b, Å	20.721(12)	11.957(13)
c, Å	17.766(10)	17.111(18)
α,°	90	90
β,°	101.240(10)	99.318(18)
γ,°	90	90
V (Å^3)	2818(3)	2032(4)
Z	4	2
Crystal size, mm	0.5 x 0.05 x 0.04	0.15 x 0.04 x 0.04
T, K	172(2)	173(2)
Ref. Coll.	50056	34680
Indep.Ref. (R_{int})	7873[0.0870]	11425[0.1489]
GOF on F^2	1.013	1.002
Final *R* indices [$I > 2\sigma(I)$]	R1 = 0.0576, wR2 = 0.1153	R1 = 0.0592, wR2 = 0.0791
R indices (all data)	R1 = 0.1211, wR2 = 0.1311	R1 = 0.1963, wR2 = 0.1110

Table 5 (continued). Crystal data and refinement data for $[Co(L^{Me})Br]BPh_4$ and $[Ni(L^{Me})Cl]BPh_4$

	$[Co(L^{Me})Br]BPh_4$	$[Ni(L^{Me})Cl]BPh_4$
Empirical Formula	$C_{50}H_{53}BBrCoN_5$	$C_{50}H_{53}BClN_5Ni$
Crystal system	Monoclinic	Monoclinic
Space Group	P2(1)/n	P2(1)/n
a, Å	12.5584(3)	12.5069(17)
b, Å	18.1423(5)	18.029(2)
c, Å	19.2187(5)	19.301(3)
α,°	90	90
β,°	96.238(1)	96.055(2)
γ,°	90	90
V (Å^3)	4352.8(2)	4327.8(10)
Z	4	4
Crystal size, mm	0.43 x 0.30 x 0.20	0.15 x 0.06 x 0.05
T, K	173(2)	173(2)
Ref. Coll.	34427	60714
Indep.Ref. (R_{int})	8558[0.0611]	9157[0.2141]
GOF on F^2	1.006	1.019
Final *R* indices [$I >$ $2\sigma(I)$]	R1 = 0.0384, wR2 = 0.0871	R1 = 0.0670, wR2 = 0.1137
R indices (all data)	R1 = 0.0549, wR2 = 0.0950	R1 = 0.1734, wR2 = 0.1443

Table 5 (continued). Crystal data and refinement data for $[Cu(L^{Me})Cl]BF_4$ and $[Cu(L^{Me})CO]PF_6$

	$[Cu(L^{Me})Cl]BF_4$	$[Cu(L^{Me})CO]PF_6$
Empirical Formula	$C_{24}H_{30}BClCuF_4N_4$	$C_{25}H_{30}CuF_6N_4OP$
Crystal system	Orthorhombic	Monoclinic
Space Group	Pna2(1)	P2(1)/n
a, Å	9.0188(5)	11.412(6)
b, Å	21.9007(14)	14.348(7)
c, Å	12.4198(7)	16.781(8)
α,°	90	90.00
β,°	90	95.398(8)
γ,°	90	90.00
V (Å^3)	2453.1(2)	2736(2)
Z	4	4
Crystal size, mm	0.52 x 0.30 x 0.28	0.18 x 0.13 x 0.04
T, K	173(2)	173(2)
Ref. Coll.	28619	57440
Indep.Ref. (R_{int})	8482[0.0525]	9522[0.0884]
GOF on F^2	1.044	1.036
Final *R* indices [$I > 2\sigma(I)$]	R1 = 0.0588, wR2 = 0.1478	R1 = 0.0551, wR2 = 0.1321
R indices (all data)	R1 = 0.0659, wR2 = 0.1552	R1 = 0.1075, wR2 = 0.1566

Table 5 (continued). Crystal data and refinement data for $[Fe(Me_6tren)Cl]BPh_4$

	$[Fe(Me_6tren)Cl]BPh_4$
Empirical Formula	$C_{38}H_{53}BClFeN_5$
Crystal system	Monoclinic
Space Group	Pc
a, Å	12.487(5)
b, Å	12.478(5)
c, Å	23.570(10)
α,°	90
β,°	90.510(7)
γ,°	90
V (Å^3)	3672(3)
Z	4
Crystal size, mm	0.20 x 0.15 x 0.10
T, K	173(2)
Ref. Coll.	63558
Indep.Ref. (R_{int})	20690[0.0623]
GOF on F^2	1.044
Final R indices [$I > 2\sigma(I)$]	R1 = 0.0744, wR2 = 0.2028
R indices (all data)	R1 = 0.0937, wR2 = 0.2151

Acknowledgements

Research advisor: Cora E. MacBeth, Ph. D

Committee members: Cora E. MacBeth, Ph. D; Craig L. Hill, Ph. D;

Simon B. Blakey, Ph. D

Group members: Matthew B. Jones, Kelly A. Kluge, Sheri Lense, Ph.D; Savita Sharma, Ph.D; Omar Villanueva

Dr. Kenneth I. Hardcastle, Dr. Rui Cao and Dr. Sheri Lense for X-ray crystallographic assistance

Dr. Shao-xiong Wu for low temperature NMR assistance

Dr. Friderick H. Strobel of Mass Spectrometry Center

Part IV. References

1. Pettinari, C.; Marchetti, F.; Drozdov, A., *Comprehensive Coordination Chemistry II* **2004**, 1, 211-251.

2. Blackman, A. G., *Eur. J. Inorg. Chem.* **2008**, (17), 2633-2647.

3. Blackman, A. G., *Polyhedron* **2005**, 24, (1), 1-39.

4. Suzuki, M., *Acc. Chem. Res.* **2007**, 40, (7), 609-617.

5. Komiyama, K.; Furutachi, H.; Nagatomo, S.; Hashimoto, A.; Hayshi, H.; Fujinami, S.; Suzuki, M.; Kitagawa, T., *Bull. Chem. Soc. Jpn.* **2004**, 77, (1), 59-72.

6. Hatcher, L. Q.; Karlin, K. D., *Adv. Inorg. Chem.* **2006**, 58, 131-184.

7. Dittler-Klingemann, A.M.; Hahn, F. E., *Inorg. Chem.* **1996**, 35, (7), 1996-1999.

8. Karlin, K. D.; Kim, E., *Chem. Lett.* **2004**, 33, (10), 1226-1231.

9. Becker, M.; Heinemann, F. W.; Schindler, S., *Chem. Eur. J.* **1999**, 5, (11), 3124-3129.

10. Wuertele, C.; Sander, O.; Lutz, V.; Waitz, T.; Tuczek, F.; Schindler, S., *J. Am. Chem. Soc.* **2009**, 131, (22), 7544-7545.

11. Lee, Y.; Park, G. Y.; Lucas, H. R.; Vajda, P. L.; Kamaraj, K.; Vance, M. A.; Milligan, A. E.; Woertink, J. S.; Siegler, M. A.; Narducci Sarjeant, A. A.; Zakharov, L. N.; Rheingold, A. L.; Solomon, E. I.; Karlin, K. D., *Inorganic Chemistry (Washington, DC, United States)* **2009**, 48, (23), 11297-11309.

12. Fry, H. C.; Lucas, H. R.; Narducci Sarjeant, A. A.; Karlin, K. D.; Meyer, G. J., *Inorganic Chemistry (Washington DC, United States)* **2008**, 47, (1), 241-256.

13. Wuertele, C.; Gaoutchenova, E.; Harms, K.; Holthausen, M. C.; Sundermeyer, J.; Schindler, S., *Angew. Chem. Int. Ed.* **2006**, 45, (23), 3867-3869.

14. Hatcher, L. Q.; Karlin, K. D., *J. Biol. Inorg. Chem.* **2004**, 9, (6), 669-683.

15. Karlin, K. D.; Hayes, J. C.; Juen, S.; Hutchinson, J. P.; Zubieta, J., *Inorg. Chem.* **1982**, 21, (11), 4106-4108.

16. Britovesk, G. J. P.; England, J.; White, A. J. P., *Inorg. Chem.* **2005**, 44, (22), 8125-8134.

17. Lim, M. H.; Rohde, J. U.; Stubna, A.; Bukowski, M. R.; Costas, M.; Ho, R. Y. N.; Munck, E.; Nam, W.; Que, L., Jr., *Proc. Natl. Acad. Sci. U. S. A.* **2003**, 100, (7), 3665-3670.

18. Jensen, M. P.; Lange, S. J.; Mehn, M. P.; Que, E. L., Jr., *J. Am. Chem. Soc.* **2003**, 125, (8), 2113-2128.

19. Que, L., Jr.; Dong, Y., *Acc. Chem. Res.* **1996**, 29, (4), 190-196.

20. Mandon, D.; Machkour, A.; Goetz, S.; Welter, R., *Inorg. Chem.* **2002**, 41, (21), 5364-5372.

21. Diebold, A.; Hagen, K.S., *Inorg. Chem.* **1998**, 37, (2), 215-223.

22. Chen, K.; Que, L., Jr., *J. Am. Chem. Soc.* **2001**, 123, (26), 6327-6337.

23. Costas, M.; Que, L., Jr., *Angew. Chem. Int. Ed.* **2002**, 41, (12), 2179-2181.

24. Cohen, N. A.; Tillman, E. S.; Thakur, S.; Smith, J. R.; Eckenhoff, W. T.; Pintauer, T.,

Macromol. Chem. Phys. **2009**, 210, (3-4), 263-268.

25. Baisch, U.; Poli, R.; *Polyhedron* **2008**, 27, (9-10), 2175-2185.

26. Pintauer, T.; Braunecker, W.; Collange, E.; Poli, R.; Matyjaszewski, K., *Macromolecules* **2004**, 37, (8), 2679-2682.

27. Schatz, M.; Becker, M.; Thaler, F.; Hampel, F.; Schindler, S.; Jacobson, R. R.; Tyeklar, Z.; Murthy, N. N.; Ghosh, P.; Chen, Q.; Zubieta, J.; Karlin, K. D., Inorg. Chem. 2001, 40,(10), 2312-2322.

28. Maiti, D.; Fry, H. C.; Woertink, J. S.; Vance, M. A.; Solomon, E. I.; Karlin, K. D., *J. Am. Chem. Soc.* **2007**, 129, (2), 264-265.

29. Lucas, H. R.; Li, L.; Narducci Sarjeant, A. A.; Vance, M. A.; Solomon, E. I.; Karlink, K. D., *J. Am. Chem. Soc.* **2009**, 131, (9), 3230-3245.

30. England, J.; Davies, C. R.; Banaru, M.; White, A. J. P.; Britovsek, G. J. P., *Adv, Synth. Catal.* **2008**, 350, (6), 883-897.

31. England, J.; Britovsek George, J. P.; Rabadia, N.; White Andrew, J. P., *Inorg, Chem* **2007**, 46, (9), 3752-3767.

32. England, J.; Gondhia, R.; Bigorra-Lopez, L.; Petersen, A. R.; White. A. J. P.; Britovsek, G. J. P., *Dalton Transactions* **2009**, (27), 5319-5334.

33. Zhang, C. X.; Kaderli, S.; Costas, M.; Kim, E. I.; Neuhold, Y. M.; Karlin, K. D.; Zuberbuehler, A. D., *Inorg. Chem.* **2003**, 42, (6), 1807-1824.

34. Jones, M. B.; MacBeth, C. E., *Inorg. Chem* **2007**, 46, (20), 8117-8119.

35. Warren, L. F., *Inorg. Chem.* **1977**, 16, (11), 2814-2819.

36. Jones, M. B.; Newell, B. S.; Hoffert, W. A.; Hardcastle, K. I.; Shores, M. P.; MacBeth, C. E., *Dalton Transactions* **2008** 39 (2), 401-410.

37. Jones, M. B.; Hardcastle, K. I.; MacBeth, C. E., Polyhedron 29, (1), 116-119.

38. Paraskevopoulou, P.; Ai, L.; Wang, Q.; Pinnapareddy, D.; Acharyya, R.; Dinda, R.; Das, P.; Celenligil-Cetin, R.; Floros, G.; Sanakis, Y.; Choudhury, A.; Rath, N. P.; Stavropoulos, P., *Inorganic Chemistry (Washington DC, United States)* **2010**, 49, (1), 108-122.

39. Celenligil-Cetin, R.; Paraskevopoulou, P.; Lalioti, N.; Sanakis, Y.; Staples, R. J.; Rath, N. P.; Stavropoulos, P., *Inorganic Chemistry (Washington DC, United States)* **2008**, 47, (23), 10998-11009.

40. Celenligil-Cetin, R.; Paraskevopoulou, P.; Dinda, R.; Lalioti, N.; Sanakis, Y.; Rawashdeh, A. M.; Staples, R. J.; Sinn, E.; Starvropoulos, P., *Eur. J. Inorg. Chem.* **2008**, (5), 673-677.

41. Celenligil-Cetin, R.; Paraskevopoulou, P.; Dinda, R.; Staples, R. J.; Sinn, E.; Rath, N. P.; Starvropouplos, P., *Inorganic Chemistry (Washingtong DC, United States)* **2008**, 47, (3), 1165-1172.

42. Borch, R. F.; Hassid, A. I., *J. Org. Chem.* **1972**, 37, (10), 1673-1674.

43. Lane, C. F., *Synthesis* **1975**, (3), 135-146.

44. Kelly, B. V.; Tanski, J. M.; Anzovino, M. B.; Parkin, G.; *J. Chem. Crystallorgr.* **2005**, 35, (12),

969-981.

45. Addison, A. W.; Rao, T. N.; Reedijk, J.; Van Rijn, J.; Verschoor, G. C., *Dalton Trans.* **1984**, (7), 1349-1356.

46. Di Vaira, M.; Orioli, P., *Inorg. Chem.* **1967**, 6, (5), 955-957.

47. Ciampolini, M.; Nardi, N., *Inorg. Chem.* **1966**, 5, (1), 41-44.

48. Colpas, G. J.; Kurmar, M.; Day, R. O.; Maroney, M. J., *Inorg. Chem.* **1990**, 29, (23), 4779-4788.

49. Wei, N.; Murthy, N. N.; Karlin, K. D., *Inorg. Chem.* **1994**, 33, (26), 6093-6100.

50. Laitar, D. S.; Mathison, C. J. N.; Davis, W. M.; Sadighi, J. P., *Inorg. Chem.* **2003**, 42, (23), 7354-7356.

51. Kretzer, R. M.; Ghiladi, R. A.; Lebeau, E. L.; Liang, H. C.; Karlin, K. D., *Inorg. Chem.* **2003**, 42, (23), 7354-7356.

52. Orpen, A. G.; Brammer, L.; Allen, F. H.; Kennard, O.; Watson, D. G.; Taylor, R., *Dalton Trans.* **1989**, (12), S1-S83.

53. Kimura, E.; Koike, T.; Kodama, M.; Meyerstein, D., *Inorg. Chem.* **1989**, 28, (15), 2998-3001.

54. Achternbosch, M.; Apfel, J.; Fuchs, R.; Kluefers, P.; Selle, A. Z., *Anorg. Allg. Chem.* **1996**, 622, (8), 1365-1373.

55. Ferguson, G.; Parvez, M., *Acta Crystallographica, Section B: Structural Crystallography and Crystal Chemistry* **1979**, B35, (9), 2207-2210.

56. Scifinder, Web version 2010 Chemical Abstracts Service: Columbus, Ohio. Calculated using Advanced Chemistry Deveplopment (ACD/Lab) Software version V8.14 (1994-2010) RN: 121-69-7, 109-06-8 and 598-56-1. In.

57. Gerdemann, C.; Eicken, C.; Krebs, B. *Acc. Chem. Res.* **2002**, *35*, 183-191

58. Chen, P.; Solomon, E. I. *J. Am. Chem. Soc.* **2004**, *126*, 4991-5000.

59. Prigge, S. T.; Kolhekar, A. S.; Eipper, B. A.; Mains, R. E.; Amzel, L. M. *Science* **1997**, *278*, 1300-1305.

60. Lucas, H. R.; Narducci Sarjeant, A. A.; Vance, M. A.; Solomon, E. I.; Karlin, K. D. *J. Am. Chem. Soc.* **2009**, *131*, 3230-3245.

61. Itoh, S.; Nakao, H.; Berreau, L. M.; Kondo, T.; Komatsu, M.; Fukuzumi, S. *J.Am. Chem. Soc.* **1998**, *120*, 2890-2899.

62. Mahapatra, S.; Halfen, J. A.; Tolman, W. B. *J. Am. Chem. Soc.* **1996**, *118*, 11575-11586.

63. Shearer, J.; Zhang, C. X.; Zakharov, L. N.; Rheingold, A. L.; Karlin, K. D. *J. Am. Chem. Soc.* **2005**, *127*, 5469-5483.

64. Shearer, J.; Zhang, C.X.; Hatcher, L.Q.; Karlin, K. D. *J. Am. Chem. Soc.* **2003**, *125*, 12670-12671.

65. Itoh, K.; Hayashi, H.; Furutachi, H.; Matsumoto, T.; Nagatomo, S.; Tosha, T.; Terada, S.;

Fujinami, S.; Suzuki, M.; Kitagawa, T. *J. Am. Chem. Soc.* **2005**, *127*, 5212-5223.

66. Wurtele, C.; Sander, O.; Lutz, V.; Waitz, T.; Tuczek, F. and Schindler, S. *J. Am. Chem. Soc.* **2009**, *131*, 7544-7545.

67. Karlin, K. D.; Wei, N.; Jung, B.; Kaderli, S.; Niklaus, P.; Zuberbuhler, A. D. *J. Am. Chem. Soc.* **1993**, *115*, 9506-9514.

68. Weitzer, M.; Schindler, S.; Brehm, G.; Schneider, S.; Hormann, E.; Jung, B.; Kaderli, S.; Zuberbuhler, A. D. *Inorg. Chem.* **2003**, *42*, 1800-1806

69. Evans, D. F., *J. Chem. Soc.* **1959**, 2003-2005.

70. Sur, S. K., *Journal of Magnetic Resonance* **1989**, 82, 169-173.

71. MacBeth, C. E.; Jones, M. B., *Abstracts of Papers, 234th ACS National Meeting, Boston, MA, United States, August 19-23, 2007* **2007**, INOR-984.

72. APEX II, 2005. Bruker AXS, Inc., Analytical X-ray Systems, 5465 East Cheryl Parkway, Madison WI 53711-5373.; 2005.

73. *SAINT Version 6.45A, 2003*. Bruker AXS, Inc., Analytical X-ray Systems, 5465 East Cheryl Parkway, Madison WI 53711-5373.; 2003.

74. Sheldrick, G. M., *Acta Crystallogr., Sect. A: Found. Crystallogr.* **2008**, A64, (1), 112-122.

75. Wilson (ed), A. J. C., *International Tables for X-ray Crystallography, Volume C.* Kynoch, Academic Publishers: Dordrecht, 1992.

76. Masarwa, A.; Rachmilovich-Calis, S.; Meyerstein, N.; Meyerstein, D. *Coord. Chem. Rev.* **2005**, 249, 1937-1943.

77. Lucas, H. R.; Li, L.; Narducci Sarjeant, A. A.; Vance, M. A.; Solomon, E. I.; Karlin, K. D., *J. Am. Chem. Soc.* **2009**, 131, 32320-3245.